a

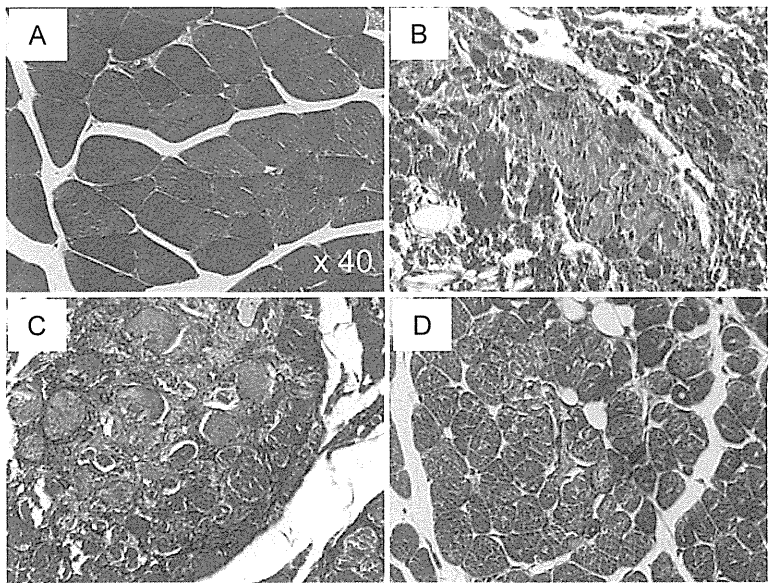

b

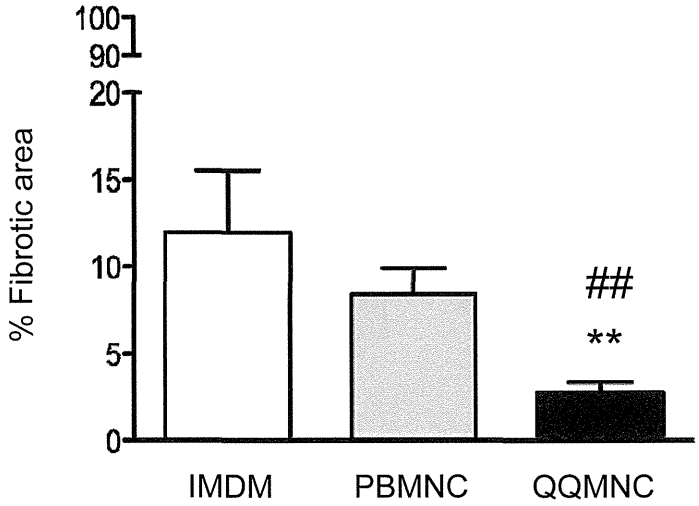

c

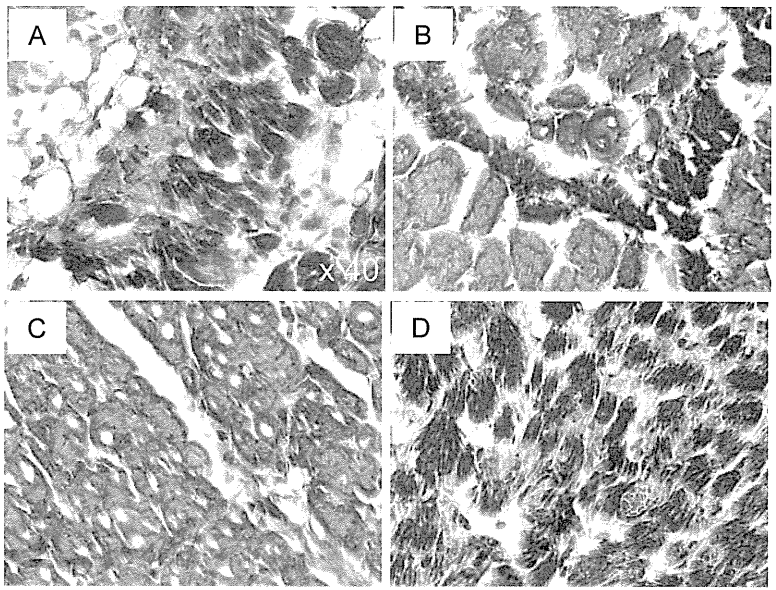
A
B
C
D
x 40

d

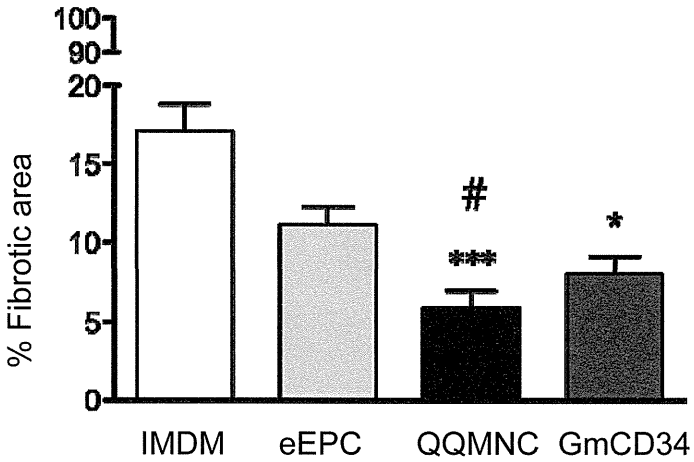
% Fibrotic area
100
90
20
15
10
5
0
#
***
*
IMDM
eEPC
QQMNC
GmCD34

a

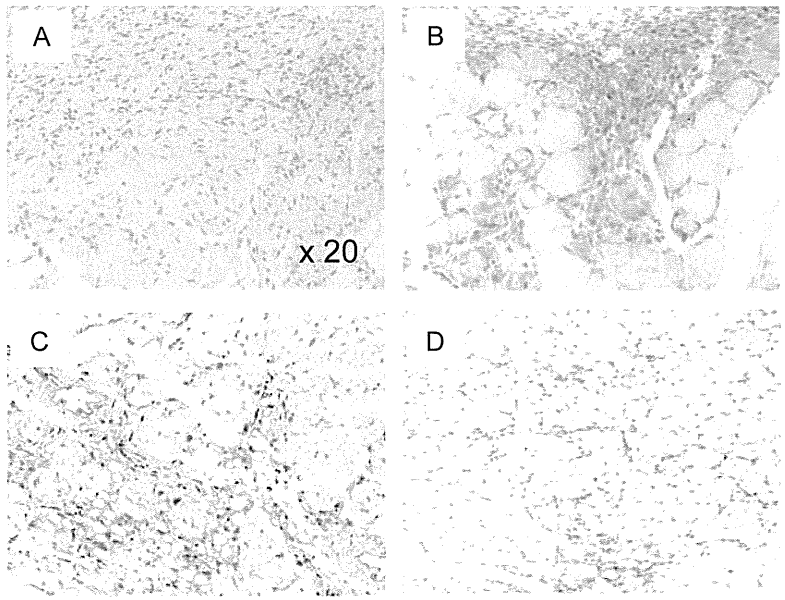
A
x 20
B
C
D

b

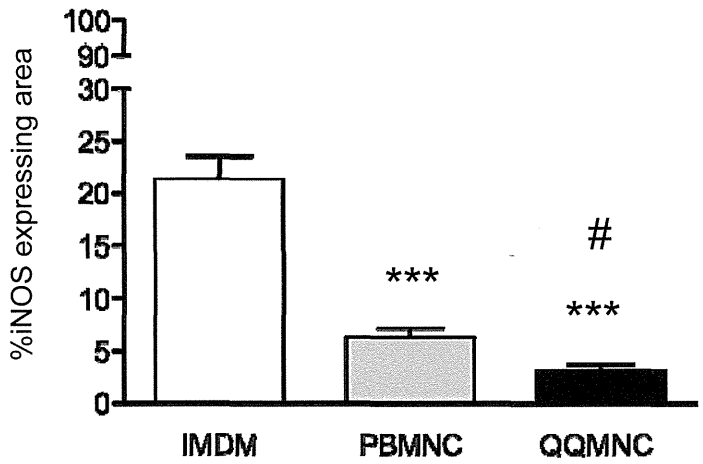
%iNOS expressing area
100
90
30
25
20
15
10
5
0
***
***
#
IMDM
PBMNC
QQMNC

c

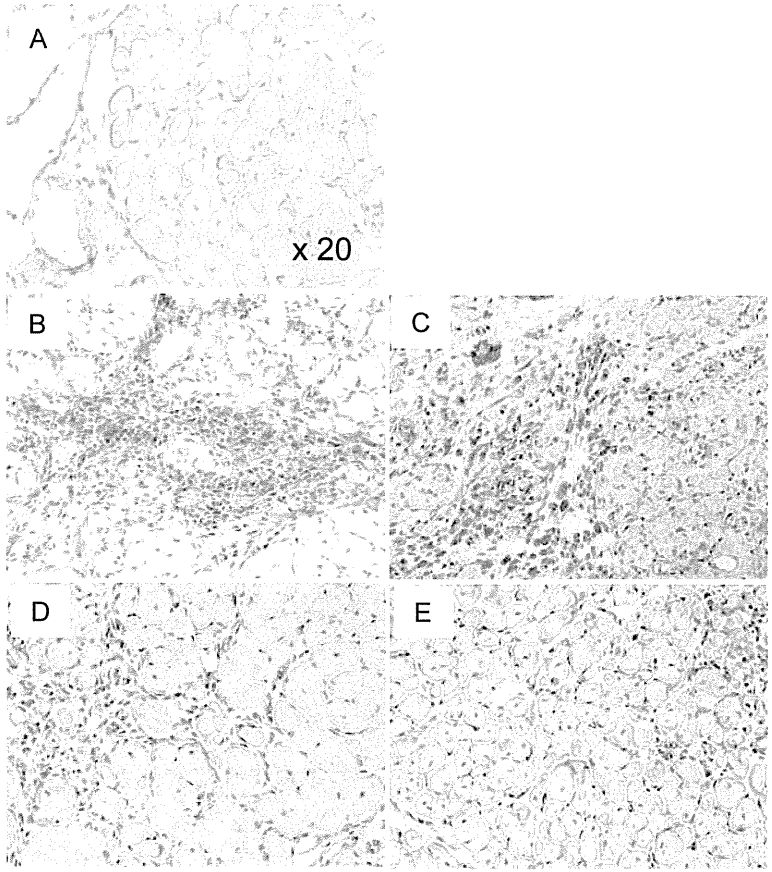
A
x 20
B
C
D
E

d

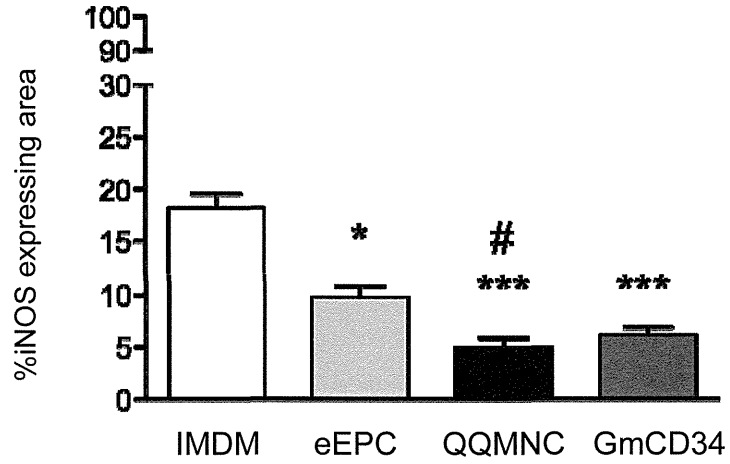
%iNOS expressing area
100
90
30
25
20
15
10
5
0
*
#
***
***
IMDM
eEPC
QQMNC
GmCD34

a

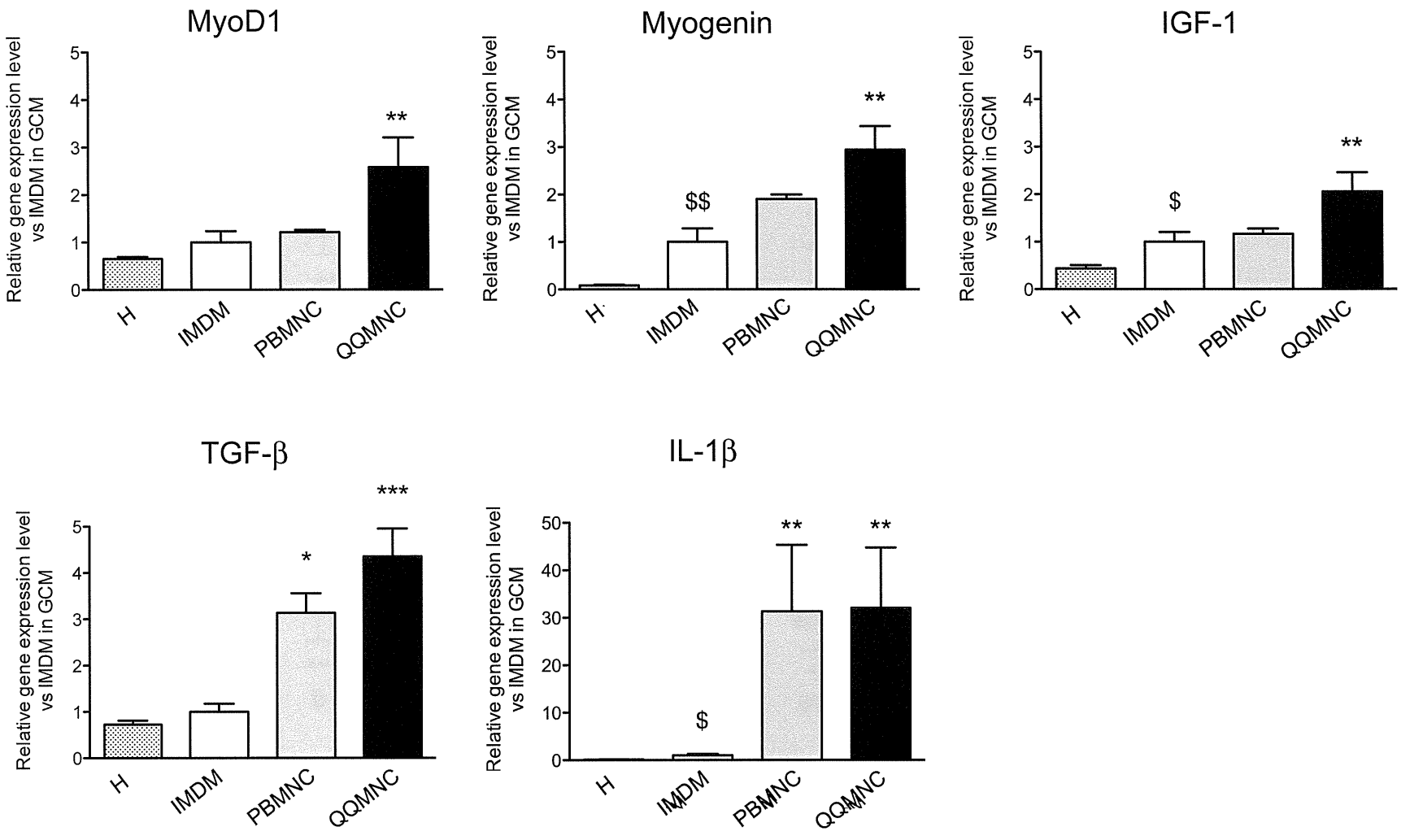
MyoD1
Myogenin
IGF-1
TGF-β
IL-1β
Relative gene expression level vs IMDM in GCM
H
IMDM
PBMNC
QQMNC
**
$$
$
*
***

b

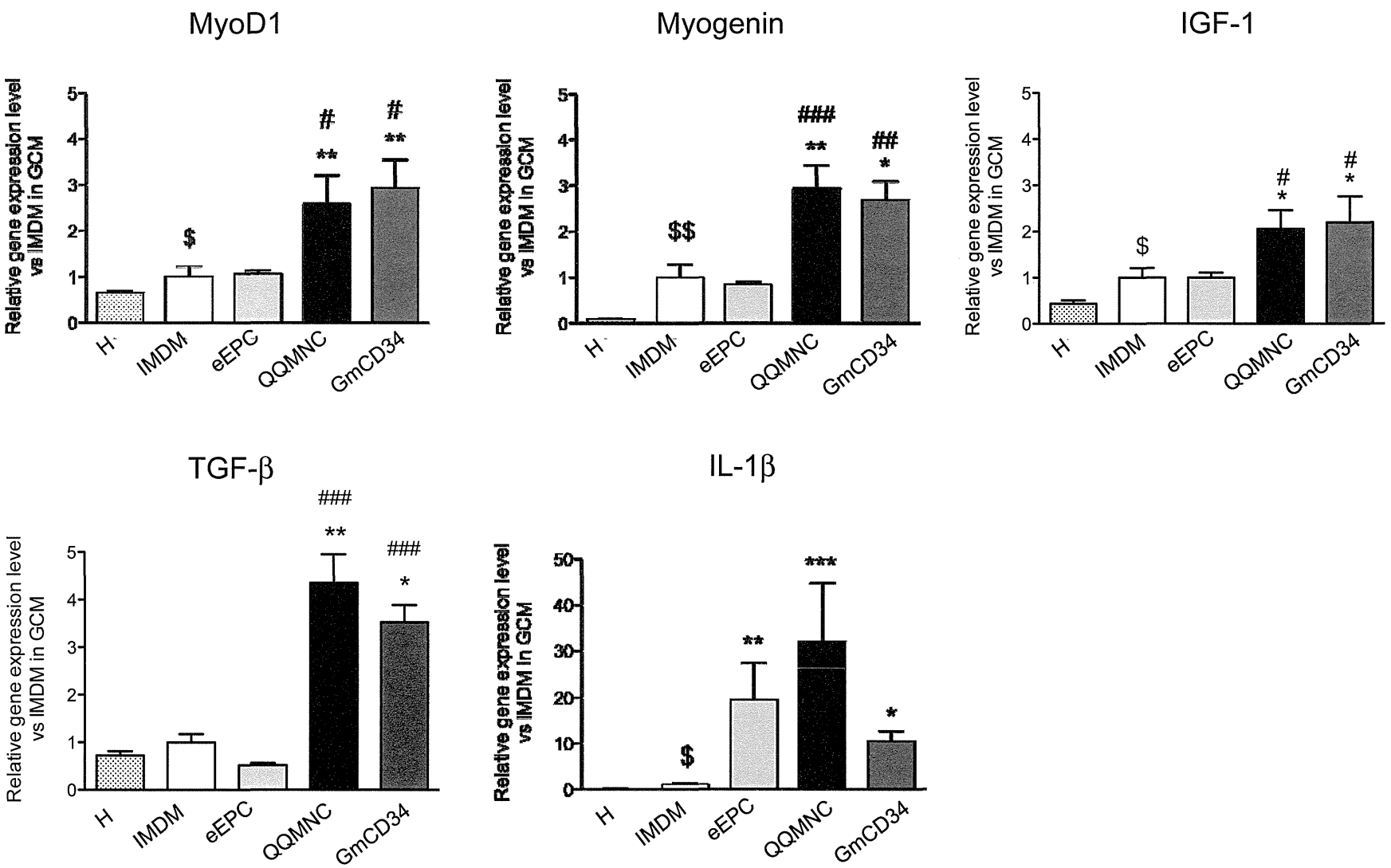
MyoD1
Myogenin
IGF-1
TGF-β
IL-1β
Relative gene expression level vs IMDM in GCM
H
IMDM
eEPC
QQMNC
GmCD34

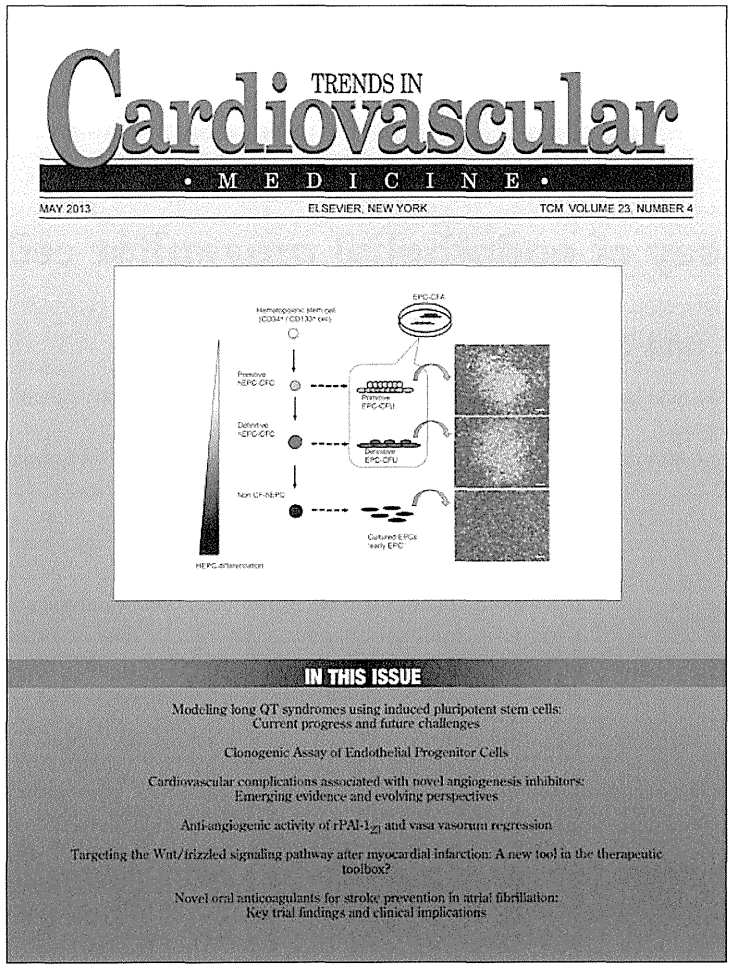

TRENDS IN CARDIOVASCULAR MEDICINE 23 (2013) 99–103

Available online at www.sciencedirect.com

SciVerse ScienceDirect

www.elsevier.com/locate/tcm

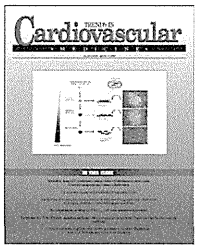

Review article

Clonogenic assay of endothelial progenitor cells

Haruchika Masuda[a], *and Takayuki Asahara*[a,b,*]

[a]*Department of Regenerative Medicine Science, Division of Basic Clinical Science, Tokai University School of Medicine, Shimokasuya, Kanagawa 259-1143, Isehara, Japan*

[b]*Vascular Regeneration Research Group, Institute of Biomedical Research and Innovation IBRI, Kobe, Japan*

ARTICLE INFO

Article history:
Received 22 June 2012
Received in revised form
12 September 2012
Accepted 13 September 2012
Available online 1 February 2013

ABSTRACT

In stem cell biology, $CD34^+$ or $CD133^+$ hematopoietic stem cells (HSCs) give rise to two types of endothelial progenitor cell (EPC) colonies: primitive and definitive EPC-colony forming units (*primitive* EPC-CFU and *definitive* EPC-CFU), which can be morphologically defined. Based on their morphology, an evaluation of the number or the ratio of each EPC colony constitutes the Endothelial Progenitor Cell Clonogenic Forming Assay (EPC-CFA), a novel assay to quantify the differentiation of colony forming EPCs. This assay system allows us to practically evaluate the vasculogenic potential of primary or cultured stem cell populations, i.e., mononuclear cells or fractionated stem cells ($CD34^+$ or $CD133^+$ cells) in peripheral blood, bone marrow, or umbilical cord blood. EPC-CFA can be used not only for basic research in vascular biology but also for evaluating the vascular reparative activity of patients with cardiovascular diseases. This review summarizes the underlying concepts and significance of the EPC-CFA in vascular biology.

Introduction

Circulating endothelial progenitor cells (EPC) can be subdivided into two categories, *hematopoietic* and *non-hematopoietic lineage* EPCs (hEPCs and non-hEPCs), after the controversy during the decade following their initial isolation (Asahara et al., 1997, 2011), as there is no definitive delineation of EPCs, no clear differentiation hierarchy, and no defined isolation protocol. hEPCs have been revealed to be derived from a pro-vasculogenic subpopulation of hematopoietic stem cells (HSCs) in the bone marrow (BM) (Asahara et al., 2011).

hEPCs have been quantified and qualified as either circulating cell populations identified by cell surface markers such as CD34, CD133, and Vascular Endothelial Growth Factor Receptor-2 (VEGFR-2) (Asahara et al., 2011), or as 'colonies' (Hill et al., 2003) using conventional EPC culture methods to produce spindle adherent cells from peripheral blood (PB), BM, or umbilical cord blood (UCB) mononuclear cells (MNCs) with endothelial growth factors and cytokines.

These assays, using conventional EPC culture protocols, are simple and satisfactory for estimating the vasculogenic properties of EPC-enriched fractions, but have recently been criticized with respect to the quality and quantity of EPCs derived from primary cells. These assays further group heterogeneous EPCs into one qualitative category, "adhesive cultured EPCs", without any hierarchical discrimination or proper characterization of contaminating cell populations, consisting mainly of hematopoietic cells (Rohde et al., 2007). Ingram et al. (2005) have demonstrated circulating endothelial differential stages, with high- and low proliferative potential-endothelial colony forming cells (HPP-ECFCs and LPP-ECFCs), using their original

*Corresponding author at: Department of Regenerative Medicine Science, Division of Basic Clinical Science, Tokai University School of Medicine, Shimokasuya, Isehara, Kanagawa 259-1143, Japan. Tel.: +11 81 463 93 1121x2521; fax: +11 81 463 95 0961.
E-mail address: asa777@is.icc.u-tokai.ac.jp (T. Asahara).

1050-1738/$ - see front matter © 2013 Elsevier Inc. All rights reserved.
http://dx.doi.org/10.1016/j.tcm.2012.09.007

culture parameters, demonstrating clonal CFUs in outgrowth EPCs, cultured adhesive EPCs, or differentiated endothelial cells (ECs). This carefully conceived culture assay system, which demonstrates thorough insight into stem cell biology, has contributed significantly to the development of EPC biology via the introduction of a differential hierarchy system for ECs.

However, this system does not identify primary circulating EPCs from PB, BM, or UCB, i.e., hEPCs, but instead isolates CFUs from cultured adhesive cells of tissue-derived ECs or EPCs, which is to say, non-hematopoietic EPCs (Asahara et al., 2011). Considering the necessity to create a defined assay to detect hEPCs qualitatively and quantitatively from primary blood samples, we have developed a new colony assay system, modifying the conventional methylcellulose assay used for stem/progenitor cell identification (Benndorf et al., 2007; Eichmann et al., 1997; Rustemeyer et al., 2007).

As we have recently reported, the present assay system discriminates two types of EPC-CFUs, morphologically identified by their respective colony cells with their specific features (Masuda et al., 2011). The first group of colony cells presents proliferative capabilities, and in a secondary semi-solid colony assay system, they are converted into the latter cell type with vasculogenic properties. The two types are defined as primitive EPC-CFUs and definitive EPC-CFUs, respectively.

The concept of EPC-CFA in hEPC differentiation cascade

Over the last decade, there have been a couple of reported EPC culture methods to identify hEPCs in circulation by the quantification of 'adhesive EPCs' from PBMNCs. These are known as the 'cultured EPC assay' and 'Hill's assay' that use endothelial cell-conditioned medium. Since then, these culture methods have been revealed to present the adhesive or aggregation features of circulating angiogenic cells (CACs), i.e., T-lymphocytes (Hur et al., 2007), monocytes/macrophages (Rehman et al., 2003), or 'early EPC' (Duan et al., 2006), indicating that these assay systems are insufficient to investigate the hEPC differentiation activity from HSCs. In contrast to conventional culture methods, EPC-CFA has been demonstrated to be a clonogenic culture system that accurately assesses the differentiation of hEPCs from HSCs. In fact, the $CD133^+$ cells of the HSC fraction in UCB in EPC-CFA generate EPC-CFUs, but not 'adhesive EPCs', as they appear in conventional culture assays. On the other hand, colony cells of definitive EPC-CFUs show the cellular phenotype of 'adhesive EPCs' in the EPC culture assay. These findings indicate that there exists a hierarchical EPC differentiation

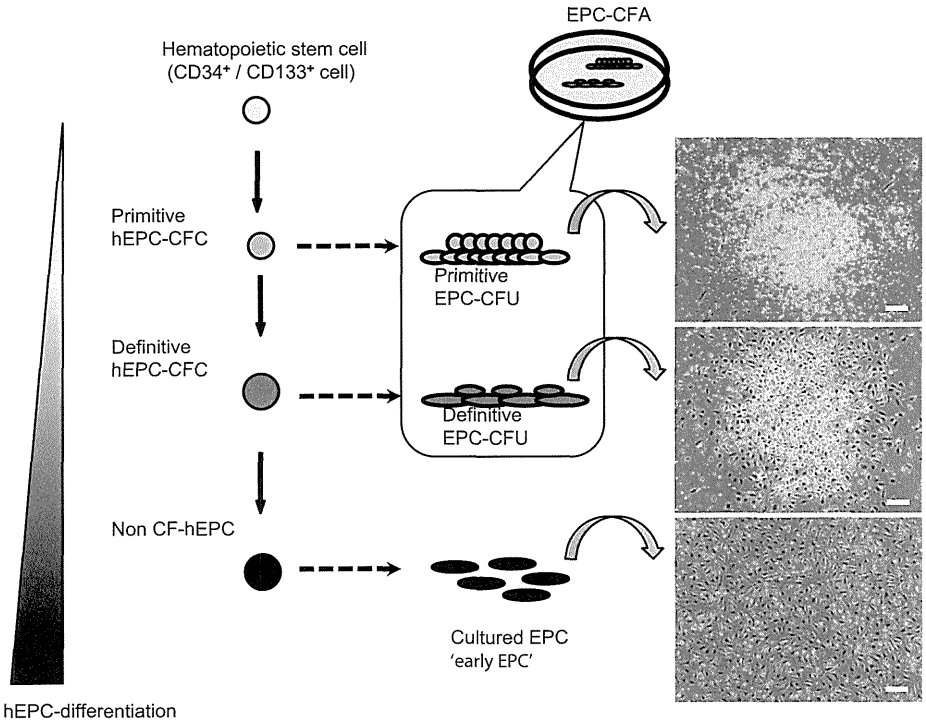

Fig. 1 – Concept of EPC-CFA to assess the hEPC differentiation cascade. hEPCs originate from HSCs. During hEPC differentiation, hEPCs loose their colony forming potential and become vasculogenic. Based on this, hEPCs exhibit individual colony forming features: primitive EPC-CFUs or definitive EPC-CFUs, which are morphologically defined as small round colony cells or spindle-like colony cells; these are respectively pro-vasculogenic or vasculogenic, thereby providing the significance to evaluate the number or frequency of each colony for the assessment of vasculogenic potential of investigated cell populations. HSC: hematopoietic stem cell; hEPC-CFC: hematopoietic EPC colony forming cell; non CF-hEPC: non colony forming hematopoietic EPC. The upper, middle, and lower pictures indicate primitive EPC-CFU, definitive EPC-CFU, or cultured EPC, respectively. Scale bar = 200 μm.

cascade in circulation that consists of each EPC colony forming cell type, primitive EPC-CFUs or definitive EPC-CFUs, at an immature phase, and then non-colony forming EPCs, i.e., 'early EPCs' at a more differentiated phase (Fig. 1).

EPC-CFA to assess colony forming EPC kinetics in hematopoietic cell population

The present assay system differentiates the two types of EPC-CFUs morphologically by identifying their respective colony cells as having small (10–20 μm) round cells and large (50–200 μm) spindle-like cells (Masuda et al., 2011). The former small round colony cells are proliferative, and in a secondary semi-solid colony assay system, the cells convert into the latter vasculogenic type, and are defined as primitive EPC-CFUs and definitive EPC-CFUs, respectively. Our findings indicate that there is a hierarchical differentiation cascade of EPC colony forming cells, allowing for quantitative enumeration of colonies and calculation of the ratio of the number of definitive EPC-CFUs to total EPC-CFUs (Fig. 2). In other words, the fundamental concept of EPC-CFA allows us to quantitatively assess each colony in terms of hEPC differentiation kinetics.

Application for basic research in vascular biology

EPC-CFA is available for primary or cultured cell populations of MNCs, and single or bulky stem cells in hematological cell populations (PB, BM, and CB), except for BM-MNCs, which include stromal cells that disturb the growth of EPC-CFUs. This universal application allows for investigation of the EPC bioactivity of proliferation or differentiation in cell populations of interest. In particular, the single stem cell fate can be analyzed by a hematopoietic and/or endothelial cell lineage commitment assay (HELIC assay) (Masuda et al., 2011), where hematopoietic CFA can be performed simultaneously with EPC-CFA in expansion cultured cells from single stem cells. The HELIC assay provides better information concerning the relationship between hematopoietic and endothelial lineages committed from HSCs (Fig. 3).

Clinical applications

Additionally, EPC-CFA is available for the evaluation of vasculogenic potential of target cells isolated from patients with cardiovascular disorders who have been reported to have a

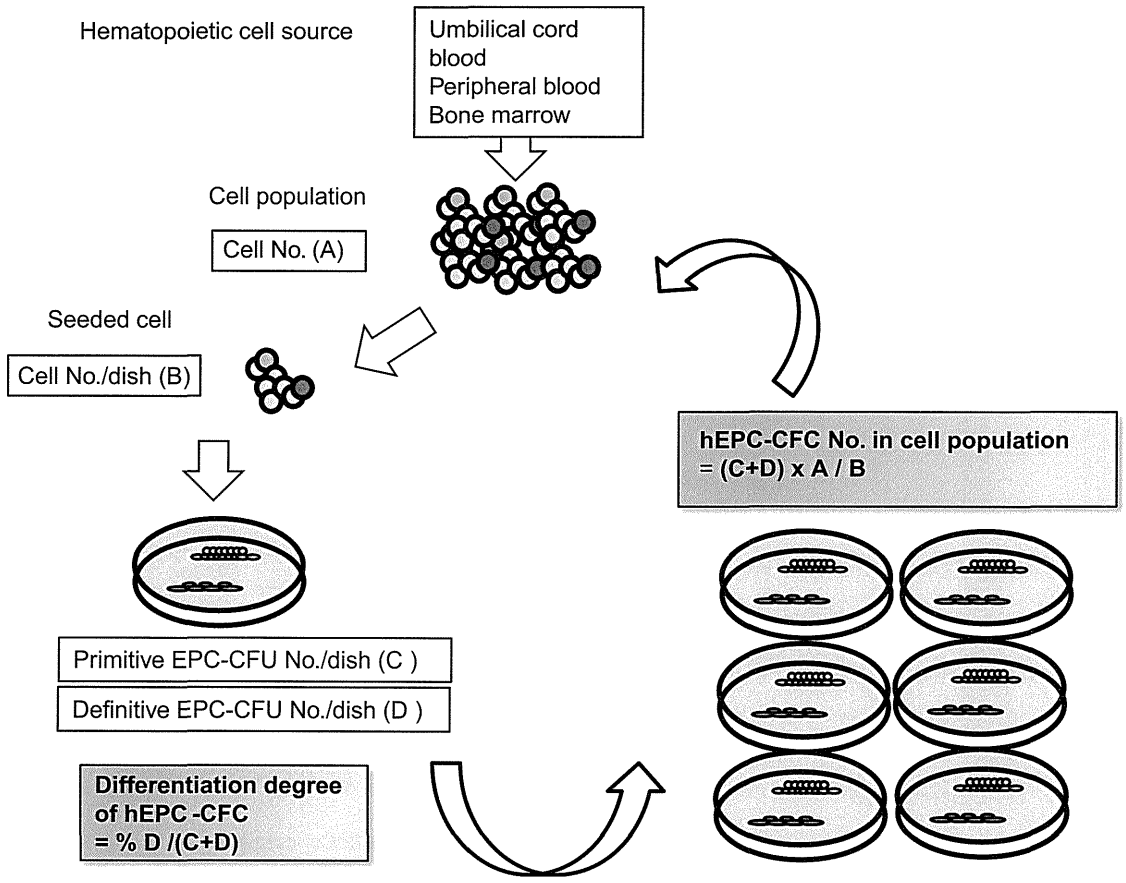

Fig. 2 – EPC-CFA to evaluate the degree of differentiation and number of hEPC-CFCs in a hematopoietic cell population. EPC-CFA allows us to evaluate the differentiation degree and number of hEPC-CFCs in investigated cell population from hematopoietic cell sources. (1) When performing EPC-CFA, the cell number (A) and seeded cell number per dish (B) of the cell population are first determined. (2) Using the counted numbers of primitive and definitive EPC-CFUs/dish (C and D), the differentiation degree is calculated as the %ratio of D to total EPC-CFUs (C + D). Further, total hEPC-CFCs in the whole cell population are simply estimated by the equation (C + D) × A/B.

reduction in EPC kinetics, i.e., mobilization, proliferation, or differentiation (Fadini et al., 2006; Hill et al., 2003). The assessment of vascular repair or regenerative capabilities in patients can thus be performed practically. Alternatively, under EPC therapy using autologous PBMNCs (Moriya et al., 2009), or PB-$CD34^+$ cells mobilized after G-CSF administration (Kawamoto et al., 2006), etc., EPC-CFA using cells from patients permits the evaluation of vasculogenic potential at the pre- or post-transplantation stage, enabling prognosis of therapeutic efficacy.

Future perspectives

For basic research into vascular biology, EPC-CFA can detect the differentiation of HSCs into the vasculogenic phase. In particular, EPC-CFA may help clarify the specific surface antigens of circulating EPC-colony forming cells, which are still elusive. Moreover, cell surface marker profiling of EPC-colony forming cells enables the direct identification of those cells in circulation by flow cytometry, thereby leading to the complete elucidation of the EPC differentiation cascade from colony forming to non-colony forming EPCs. Such a direct analysis of the EPC differentiation cascade by flow cytometry, based on EPC-CFA, would result in a more objective and time-saving methodology, whereas EPC-CFA requires the time-consuming need to grow EPC-CFUs, it eliminates the training needed for quantification of those colonies under present circumstances.

Conclusion

EPC-CFA permits the determination of the fate of circulating hEPCs, based on a numerical assessment of their hierarchical adhesive clonogenicity, providing a novel and powerful tool not only to investigate the significance of EPC differentiation in vascular biology but also to evaluate the vasculogenic potential of patients in clinical situations.

Disclosures

None.

Acknowledgments

We thankfully accepted the outstanding technical supports from the Teaching and Research Support Center of Tokai University School of Medicine and Ms. Tomoko Shizuno, as well as

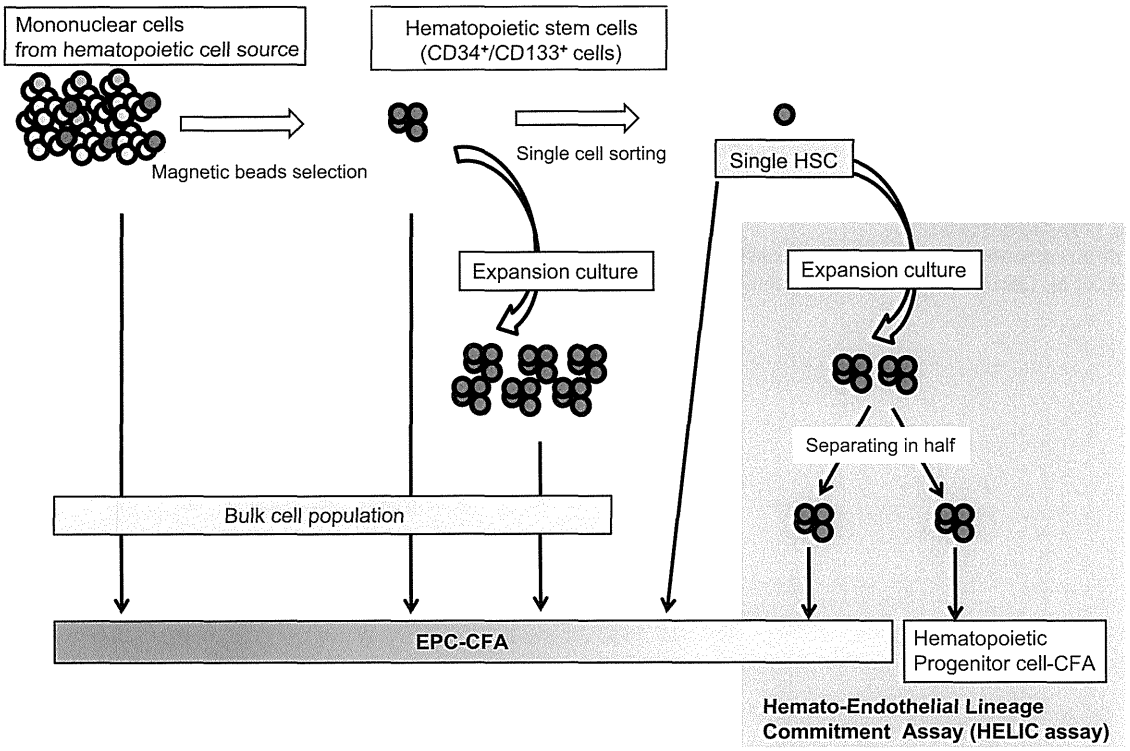

Fig. 3 – Application of EPC-CFA for primary or expansion cultured cell populations. EPC-CFA is applicable for primary or expansion cultured cells, not only for bulk non-selected MNCs or selected $CD34^+/CD133^+$ cells, but also for single selected $CD34^+/CD133^+$ cells. In particular, the Hemato-Endothelial lineage commitment assay (HELIC assay), which is applicable for EPC-CFA, uses single hematopoietic stem cells to analyze their commitment into hematopoietic and/or endothelial lineages. In brief, EPC-CFA and a conventional hematopoietic progenitor cell-CFA can be performed practically by using half of each expansion of the cultured cells from a single hematopoietic stem cell. Subsequently, the cell fate of the single stem cells into endothelial and/or hematopoietic cell lineages is quantitatively evaluated by analyzing the frequency of the stem cell generating EPC-CFUs in EPC-CFA and/or hematopoietic lineage-CFUs (e.g., erythrocyte-CFU, granulocyte/macrophage-CFU and monocyte/macrophage-CFU) in hematopoietic progenitor cell-CFA.

Ms. Sachie Ota for her secretarial assistance. This work was supported by grants from the Riken Center for Developmental Biology Collaborative Research Fund (08001475), Kobe for T.A.; National Institutes of Health (HL53354 and HL57516), Bethesda, MD for T.A.; the Ministry of Health, Labor and Welfare (H14-trans-001, H14-trans-002, H17-trans-002, H17-trans-014, and H20-regenerative medicine-general-001), Japan for T.A.; the Ministry of Education, Culture, Sports, Science and Technology (Basic Research Grant 22590796 for H.M., and Program for the Strategic Research Foundation at Private Universities, S1201001 for T.A. and H.M.), Japan.

REFERENCES

Asahara T, Kawamoto A, Masuda H. Concise review: circulating endothelial progenitor cells for vascular medicine. Stem Cells 2011;29(11):1650–5.

Asahara T, Murohara T, Sullivan A, Silver M, van der Zee R, Li T, et al. Isolation of putative progenitor endothelial cells for angiogenesis. Science 1997;275(5302):964–7.

Benndorf RA, Gehling UM, Appel D, Maas R, Schwedhelm E, Schlagner K, et al. Mobilization of putative high-proliferative-potential endothelial colony-forming cells during antihypertensive treatment in patients with essential hypertension. Stem Cells and Development 2007;16(2):329–38.

Duan HX, Cheng LM, Wang J, Hu LS, Lu GX. Angiogenic potential difference between two types of endothelial progenitor cells from human umbilical cord blood. Cell Biology International 2006;30(12):1018–27.

Eichmann A, Corbel C, Nataf V, Vaigot P, Breant C, Le Douarin NM. Ligand-dependent development of the endothelial and hemopoietic lineages from embryonic mesodermal cells expressing vascular endothelial growth factor receptor 2. Proceedings of the National Academy of Sciences of the United States of America 1997;94(10):5141–6.

Fadini GP, de Kreutzenberg SV, Coracina A, Baesso I, Agostini C, Tiengo A, et al. Circulating $CD34^+$ cells, metabolic syndrome, and cardiovascular risk. European Heart Journal 2006;27(18):2247–55.

Hill JM, Zalos G, Halcox JP, Schenke WH, Waclawiw MA, Quyyumi AA, et al. Circulating endothelial progenitor cells, vascular function, and cardiovascular risk. New England Journal of Medicine 2003;348(7):593–600.

Hur J, Yang HM, Yoon CH, Lee CS, Park KW, Kim JH, et al. Identification of a novel role of T cells in postnatal vasculogenesis: characterization of endothelial progenitor cell colonies. Circulation 2007;116(15):1671–82.

Ingram DA, Caplice NM, Yoder MC. Unresolved questions, changing definitions, and novel paradigms for defining endothelial progenitor cells. Blood 2005;106(5):1525–31.

Kawamoto A, Iwasaki H, Kusano K, Murayama T, Oyamada A, Silver M, et al. CD34-positive cells exhibit increased potency and safety for therapeutic neovascularization after myocardial infarction compared with total mononuclear cells. Circulation 2006;114(20):2163–9.

Masuda H, Alev C, Akimaru H, Ito R, Shizuno T, Kobori M, et al. Methodological development of a clonogenic assay to determine endothelial progenitor cell potential. Circulation Research 2011;109(1):20–37.

Moriya J, Minamino T, Tateno K, Shimizu N, Kuwabara Y, Sato Y, et al. Long-term outcome of therapeutic neovascularization using peripheral blood mononuclear cells for limb ischemia. Circulation. Cardiovascular Interventions 2009;2(3)245–54.

Rehman J, Li J, Orschell CM, March KL. Peripheral blood "endothelial progenitor cells" are derived from monocyte/macrophages and secrete angiogenic growth factors. Circulation 2003;107(8):1164–9.

Rohde E, Bartmann C, Schallmoser K, Reinisch A, Lanzer G, Linkesch W, et al. Immune cells mimic the morphology of endothelial progenitor colonies in vitro. Stem Cells 2007;25(7):1746–52.

Rustemeyer P, Wittkowski W, Greve B, Stehling M. Flow-cytometric identification, enumeration, purification, and expansion of $CD133^+$ and $VEGF\text{-}R2^+$ endothelial progenitor cells from peripheral blood. Journal of Immunoassay and Immunochemistry 2007;28(1):13–23.

ORIGINAL ARTICLE

Quality-Control Culture System Restores Diabetic Endothelial Progenitor Cell Vasculogenesis and Accelerates Wound Closure

Rica Tanaka,[1,4] Max Vaynrub,[2] Haruchika Masuda,[1] Rie Ito,[1] Michiru Kobori,[1] Muneo Miyasaka,[3] Hiroshi Mizuno,[4] Stephen M. Warren,[2] and Takayuki Asahara[1]

Delayed diabetic wound healing is, in part, the result of inadequate endothelial progenitor cell (EPC) proliferation, mobilization, and trafficking. Recently, we developed a serum-free functional culture system called the quality and quantity culture (QQc) system that enhances the number and vasculogenic potential of EPCs. We hypothesize that QQc restoration of diabetic EPC function will improve wound closure. To test this hypothesis, we measured diabetic c-kit$^+$Sca-1$^+$lin$^-$ (KSL) cell activity in vitro as well as the effect of KSL cell–adoptive transfer on the rate of euglycemic wound closure before and after QQc. KSL cells were magnetically sorted from control and streptozotocin-induced type I diabetic C57BL6J bone marrow. Freshly isolated control and diabetic KSL cells were cultured in QQc for 7 days and pre-QQc and post-QQc KSL function testing. The number of KSL cells significantly increased after QQc for both diabetic subjects and controls, and diabetic KSL increased vasculogenic potential above the fresh control KSL level. Similarly, fresh diabetic cells form fewer tubules, but QQc increases diabetic tubule formation to levels greater than that of fresh control cells ($P < 0.05$). Adoptive transfer of post-QQc diabetic KSL cells significantly enhances wound closure compared with fresh diabetic KSL cells and equaled wound closure of post-QQc control KSL cells. Post-QQc diabetic KSL enhancement of wound closure is mediated, in part, via a vasculogenic mechanism. This study demonstrates that QQc can reverse diabetic EPC dysfunction and achieve control levels of EPC function. Finally, post-QQc diabetic EPC therapy effectively improved euglycemic wound closure and may improve diabetic wound healing. ***Diabetes* 62:3207–3217, 2013**

Although blood supply is essential for tissue viability, new blood vessel formation is critical for tissue recovery, regeneration, and repair. Postnatal new blood vessel formation was long thought to be restricted to angiogenesis, the sprouting of new blood vessels from existing vascular structures. However, in 1997, we demonstrated that the de novo formation of new blood vessel derived from bone marrow (BM)-derived cells (i.e., vasculogenesis) is an important part of postnatal healing (1–3). The BM-derived endothelial progenitor cells (EPCs) are precursors of endothelial cells (ECs) and are characterized by their surface expression of KDR, CD133, and CD34 for humans and of lineage-negative c-kit$^+$Sca-1$^+$ (KSL) cells for murine BM cells (4–6).

After injury, locally derived circulating factors mobilize EPCs from their endosteal BM niche. Circulating BM-derived EPCs traffic to the site of injury, experience diapedesis, cluster, tubulize, and canalize to form nascent vessels that inosculate with the existing vasculature (7,8). EPCs have been shown to revascularize numerous ischemic tissues, including myocardium (i.e., myocardial infarction), brain (i.e., cerebral infarction), and skin (i.e., cutaneous wounding) (9,10). Whereas BM-derived EPCs contribute to only 25% of newly formed endothelium in healing tissues, when EPC function is impaired there are marked deficits in tissue repair mechanisms (11,12).

Compared with nondiabetic patients, diabetic EPCs have impaired proliferation, adhesion, migration, and differentiation (13–15). Although the pathogenesis of impaired diabetic wound healing is multifactorial, EPC dysfunction plays a central role (16,17). These intrinsic diabetic EPC vasculogenic impairments may result in >83,000 amputations each year and a postamputation 3-year mortality rate of 75.9% (18). In preclinical studies, the administration of exogenous EPCs has improved ventricular function after myocardial ischemia (19,20), enhanced neuronal recovery after cerebral vascular occlusion, and accelerated restoration of blood flow to ischemic limbs (13,16,17,21–23). Based on these exciting results, we have conducted a phase 3 clinical trial of autologous granulocyte colony-stimulating factor–mobilized peripheral blood EPC therapy for nonhealing diabetic foot patients (24). The results demonstrated that more successful therapeutic results were seen in patients receiving high-vasculogenic EPCs. From these results, we hypothesize that successful autologous diabetic EPC therapy relies on the vasculogenic function of transplanted EPCs and speculate that the intrinsic diabetic EPC dysfunction will limit the efficacy of the therapeutic strategy (25,26).

Recently, our group established a serum-free quality and quantity culture (QQc) system (containing stem cell factor, thrombopoietin, vascular endothelial growth factor, interleukin-6, and Flt-3 ligand) that enhances the vasculogenic potential of EPCs (27). We hypothesize that QQc can reverse the detrimental effects of diabetes-induced EPC dysfunction and can supply a sufficient number of functional EPCs for adoptive autologous cell–based therapy for diabetic patients. In the current study, we tested this hypothesis.

RESEARCH DESIGN AND METHODS

Diabetic mouse model. C57BL/6J male mice aged 8–10 weeks and weighing 20–25 g were purchased from Crea Japan (Kawasaki, Japan) and The Jackson

From the [1]Division of Regenerative Medicine, Department of Basic Clinical Science, Tokai University School of Medicine, Kanagawa, Japan; the [2]Department of Plastic Surgery, Institute of Reconstructive Plastic Surgery Laboratories, New York University Medical Center, New York, New York; the [3]Department of Plastic and Reconstructive Surgery, Juntendo University School of Medicine, Tokyo, Japan; and the [4]Department of Plastic Surgery, Tokai University School of Medicine, Kanagawa, Japan.

Corresponding authors: Takayuki Asahara, asa777@is.icc.u-tokai.ac.jp, and Stephen M. Warren, stephen.warren.md@gmail.com.

Received 28 November 2012 and accepted 7 May 2013.

DOI: 10.2337/db12-1621

Laboratory (Bar Harbor, ME). Obliteration of pancreatic β-cells was achieved with intraperitoneal injections of 50 mg/kg streptozotocin (STZ; Sigma-Aldrich, St. Louis, MO) in 50 mmol/L sodium citrate buffer (pH 4.5) for 5 consecutive days (28). Ten days after the initial injection, mice with a blood glucose level >300 mg/dL were deemed diabetic, whereas those with a level <300 mg/dL received an additional 3 days of STZ injections (50 mg/kg). Mice were considered diabetic if they maintained glucose levels >300 mg/dL for at least 4 weeks before the date of wounding. Control mice received intraperitoneal injections at the same time points with an equal volume of 50 mmol/L sodium citrate buffer. A total of 200 mice were used in this experiment (n = 100 per group). All procedures were conducted in accordance with the guidelines set forth by the committee of Ethical Animal Care and Use at Tokai University School of Medicine and the Institutional Animal Care and Use Committee at New York University Medical Center.

BM progenitor cell isolation. BM cells were harvested from diabetic and control mouse femurs and tibias as previously described (7). Mononuclear cells were washed with PBS-EDTA, and erythrocytes were removed by ammonium chloride hemolyzation and stained with a lineage-positive antibody cocktail containing CD45R/B220, TER119, CD3e, CD11b, Ly-6G, and Ly6C (Gr-1) for 20 min at 4°C (all antibodies obtained from BD PharMingen, San Diego, CA). After labeling the lineage-positive antibodies with biotin-labeled magnetic beads, cells underwent a negative selection process with a magnetic cell sorting system. Lineage-negative cells were counted and then incubated with rat fluorescein isothiocyanate antimouse Ly-6A/E (Sca-1; BD PharMingen) and rat phycoerythrin CD117 (c-kit; BD PharMingen) for 20 min at 4°C, washed three times, and resuspended in 20% Iscove modified Dulbecco medium (Gibco, Carlsbad, CA). Fluorescein isothiocyanate–conjugated Sca-1 and phycoerythrin-conjugated c-kit double-positive cells (KSL cells) then were obtained by fluorescent-activated cell sorting.

Serum-free QQc. Diabetic and control BM KSL cells were isolated as described, and 1×10^3 cells were placed in each well of a 24-well plate (BD Falcon, Bedford, MA) and cultured in QQc for 7 days as previously described (27). Briefly, QQc is an optimized growth factor/cytokine combination (20 ng/mL thyroid peroxidase, 20 ng/mL interleukin-6, 100 ng/mL SCF, 100 ng/mL Flt-3 ligand, and 50 ng/mL vascular endothelial growth factor; all from Peprotech, Rocky Hills, NJ) serum-free stem span (Stem Cell Technologies) media. After 7 days of QQc, control KSL cells were termed C_{QQc} and diabetic KSL cells were termed DM_{QQc}. Growth in QQc has been shown to dramatically expand and enhance the vasculogenic potential of EPCs.

EPC colony-forming assay of KSL population. The vasculogenic potential of diabetic and control BM KSL cells was assessed using the EPC colony-forming assay as previously described (6,29,30). EPC colony-forming assay is designed to distinguish total EPC colony-forming units (tEPC-CFUs) into two different types of EPC-CFUs: primitive (small cell) and definitive (large cell). The primitive EPC-CFU (pEPC-CFUs) is a predominantly proliferative population of cells and the definitive EPCs-CFU (dEPC-CFU) is a predominantly vasculogenic population with greater adhesion, migration, and differentiation and tabularization potential. Briefly, a total of 500 BM KSL cells per dish were seeded into a 35-mm hydrophilic tissue culture dish. Seven days later, tEPC-CFUs, pEPC-CFUs, and dEPC-CFUs were counted by two investigators who were blinded to the experimental conditions. Experiments were performed in triplicate.

Tube formation assay. Tubule formation assay was performed by adding Biocoat Matrigel (Becton Dickinson; Franklin Lakes, NJ) into 24-well plates and incubating in a CO_2-free incubator at 37°C for 30 min. The same lot of Matrigel was used for all experiments. The gels were then overlaid with 3×10^3 fresh and expanded diabetic and control cells cocultured with 1×10^4 endothelial cells suspended in culture medium and incubated at 37°C in an atmosphere of 5% CO_2. The well cultured with endothelial cells only was used as a control. After 12 h of incubation, gels were examined by using a phase-contrast microscope equipped with a digital camera (Nikon eclipse TE2000-U; Nikon, Melville, NY). A blinded observer measured the total number of tube-like structures per high-power field (HPF) in five random fields.

Quantitative real-time PCR. Total RNA from 2×10^4 diabetic and control KSL cells was extracted using the RNeasy Micro kit (Qiagen, Basel, Switzerland) based on the manufacturer's protocol, and reverse-transcription was performed using high-capacity cDNA reverse-transcription kit (Applied Biosystems, Foster City, CA). The transcription reaction was performed at 37°C for 2 h. The obtained cDNA was amplified using the reaction mixture of TaqMan FAST Universal PCR Master Mix (Applied Biosystems). The following TaqMan probes (Applied Biosystems) were used: 18S rRNA (ribosomal RNA control reagents 4308329), endothelial growth factor (Mm00438696_m1; Egf), hepatocyte growth factor (Mm01135193_m1; Hgf), fibroblast growth factor-2 (Mm00433287_m1; Fgf2), fibroblast growth factor-7 (Mm00433291_m1; Fgf7), von Willebrand factor (Mm00550376_m1; vWF), CD29 (Mm0125320_m1; Itgb1), and Flk-1 (Mm0122419_m1; Kdr). The PCR mixtures were preincubated at 95°C for 20 s, followed by 40 cycles of 95°C for 3 s and 62°C for 30 s by ABI 7500 FAST (Applied Biosystems). The real-time data were analyzed by change (Δ) in threshold cycle (Ct) method. The ΔCt was calculated as (gene of target Ct) − (18S rRNA Ct). The relative quantity of mRNA of the target gene was determined by the ΔCt calculation $2^{-\Delta Ct}$.

Wound model and KSL adoptive cellular therapy. To reduce the confounding variables that would affect KSL function in a diabetic wound, we first used 8- to 10-week-old euglycemic C57BL/6J male mice (n = 45; 3 per experimental group in triplicates) as recipients for diabetic and control KSL therapy (31). To verify the efficacy of QQc diabetic cells in diabetic wound healing, a diabetic STZ mouse wound model was similarly prepared. Briefly, each mouse was anesthetized and depilated, and one set of bilateral 6-mm punch biopsy specimens was excised on the dorsum. Excisions were full-thickness, including the hypodermis and panniculus carnosum. India ink was applied intradermally at the margins to permanently mark the wound edge. A silicone stent (Grace Bio-Laboratories, Bend, OR) with an 8-mm inner diameter was sutured with 5–0 nylon (Ethicon, Somerville, NJ) around each wound to minimize skin contracture and to ensure healing by secondary intention. On postoperative day 3, a 1-mL syringe with a 30-gauge needle was used to inject 25 μL saline, 2×10^4 freshly isolated control KSL, 2×10^4 freshly isolated diabetic KSL, 2×10^4 post-QQc control KSL, or 2×10^4 post-QQc diabetic KSL (QD) into the center of the muscle at the base of the wound. The wounds were covered with Tegaderm to prevent the cells from leaking and drying.

Wound photographs were acquired with a 7-megapixel digital camera (Canon USA, Lake Success, NY) from a distance of 6.5 cm, with the lens oriented parallel to the wound. Wound area was measured digitally (Photoshop CS3; Adobe Systems, San Jose, CA) and calibrated against the internal diameter of the silicon stent to correct for magnification, perspective, or parallax effects. Percent wound closure {1 − [(wound area)/(original wound area)]} was measured photogrammetrically on days 0, 3, 7, 10, 14, 18, and 21.

Wound harvest. Wounds were harvested from killed animals at postoperative days 7, 14, and 21 (n = 4 per group at each time point). A full-thickness excision including 3 mm beyond the margin of the original wound edge (demarcated with India ink) was performed. Each wound was bisected, and one-half of the wound was frozen in optimal cutting temperature compound for cryosectioning. The other half was fixed in 100% methanol and embedded in paraffin. Sections were cut from the central region of the wound at a thickness of 5 μm. Before staining, paraffin sections were deparaffinized and rehydrated by successive passages through xylene and decreasing concentrations of ethanol.

Van Gieson stain for wound maturity. Wound maturity can be quantified with Van Gieson staining protocol, which simultaneously stains mature collagen deep red and stains immature collagen pink (32). Horizontal sections were cut from each specimen at each time point. Paraffin sections were processed with staining solution as described previously (33). Sections were imaged and digitized in their entirety at 200× resolution with an Aperio ScanScope GL scanning optical microscope (Aperio Technologies, Vista, CA). Images were then analyzed with Adobe Photoshop CS3 (Adobe Systems). Percentage mature collagen was quantified by measuring the total pixel area of the wound and the percentage of pixels therein that were consistent in color with mature collagen. Lateral wound margins were identified at the border of the panniculus carnosum layer.

CD31 staining for vascularity and proliferating cell nuclear antigen staining for cellular proliferation. Paraffin sections were incubated in either CD31 (an endothelial marker) or proliferating cell nuclear antigen (PCNA; a nuclear marker for proliferation) (both from Cell Signaling Technology, Danvers, MA) antibodies, washed, and stained with DAB (Vector Laboratories, Burlingame, CA). Slides were examined under 200× magnification and captured as digital images (Olympus BX51 microscope and DP12 camera). In CD31-labeled sections, patent vessels were tallied, and numeral density was reported as vessels per 200× field. Cross-sectional area of each vessel was obtained with Adobe Photoshop CS3 and reported as total cross-sectional area normalized to wound area as well as average cross-sectional area per vessel. In PCNA-labeled sections, nuclei exhibiting positive PCNA staining were tallied and reported as cells per 200× field.

Green fluoroscent protein and vWF costaining. To follow the adoptively transferred cell trafficking, BM-KSL cells from diabetic and controls were isolated from 8- to 10-week-old green fluorescent protein (GFP)-expressing C57BL6 mice (CLEA Japan) as described. The KSL cells were cultured in QQc medium for 1 week as described; 2×10^4 GFP-KSL cells were injected into 8- to 10-week-old euglycemic C57BL/6J male mice as described. Wounds were harvested from killed animals at postoperative days 7, 14, and 21 (n = 4 per group at each time point) as described. Tissue sections were fixed in 4% paraformaldehyde overnight at 4°C, processed through 100% ethanol and xylenes, and embedded in paraffin. To enhance GFP expression, samples were incubated with a 1:300 dilution of anti-GFP mouse polyclonal antibody (Invitrogen) for 1 h at room temperature, washed, and stained with DAB (DOTITE). For vWF staining, the sections were further treated with 1:300 dilution anti-vWF rabbit polyclonal antibody (DAKO) for 4°C overnight and washed and blocked in 5% normal sheep serum for 5 min followed by anti-rabbit IgG alkaline phosphatase-streptavidin

complex (NICHIREI). The double-stained images with vWF images were obtained with the same equipment as described. Dual-filter images were superimposed to illustrate GFP trafficking and wound vascular architecture.

Statistical analysis. All data are presented as the mean ± SD. A Kruskal-Wallis one-way ANOVA with Tukey-Kramer post hoc analysis was performed when comparisons involved more than two groups. Mann-Whitney test was used for pairwise comparisons. Significance was considered at $P < 0.05$. The number of animals in each group was determined with an a priori power analysis using a standard for adequacy of 80% to reject the null hypothesis of zero correlation using G*Power.

RESULTS

QQc restores growth and vasculogenic potential of diabetic EPCs. Because ex vivo expansion is an important step in adoptive cellular therapy, we measured the effects of QQc on KSL proliferation. After 7 days of QQc, the C_{QQc} population increased 338.2- ± 260.7-fold (Fig. 1*A*). Similarly, after 7 days of QQc, the DM_{QQc} population increased 329.0- ± 125.7-fold (Fig. 1*A*). There was no

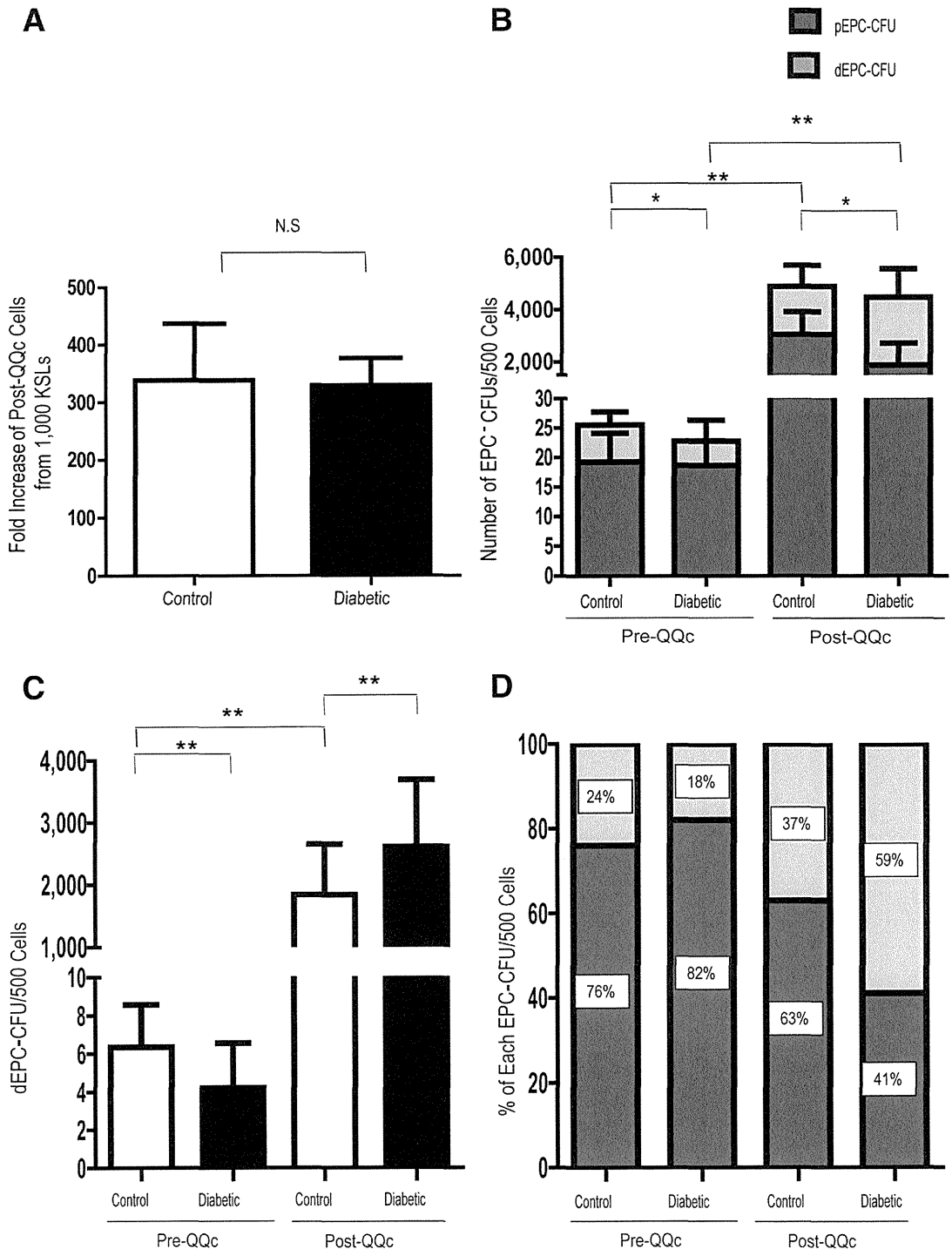

FIG. 1. QQc restores growth and vasculogenic potential of diabetic progenitor cells to more than the level of controls. *A*: Fold increase of control and diabetic post-QQc cells. *B*: The frequency of EPC-CFU production from pre-QQc and post-QQc control and diabetic KSL cells. *C*: The frequency of DEPC-CFU production from pre-QQc and post-QQc control and diabetic KSL cells. *D*: The percent of pEPC-CFUs and dEPC-CFUs from total EPC-CFUs. *$P < 0.05$; **$P < 0.01$. $n = 3$ dishes/group for 4 trials. NS, not significant.

significant difference ($P = 0.6$) in the QQc cellular expansion of diabetic and control KSL cells.

Because QQc restored ex vivo diabetic KSL expansion to control rates, we assessed the effects of QQc on the vasculogenic potential of diabetic KSL cells using EPC colony-forming assay. Before expansion, diabetic KSL cells had similar numbers of pCFUs (19.2 ± 4.9 vs. 18.6 ± 04.2; $P = 0.5$) but significantly fewer tCFUs (22.7 ± 5.2 vs. 25.0 ± 3.8; $P < 0.01$) and dEPC-CFUs (4.2 ± 2.3 vs. 6.3 ± 2.2; $P < 0.01$) compared with control KSL cells. After QQc, the number of diabetic tEPC-CFUs (4,469 ± 1,593; $P < 0.01$), pEPC-CFUs (1,862 ± 842; $P < 0.01$), and dEPC-CFUs (2,607 ± 1,084; $P < 0.01$) increased significantly from pre-QQc levels, as did the number of diabetic tEPC-CFUs (4,469 ± 1,593 vs. 4,884 ± 1,495; $P = 0.4$), and dEPC-CFUs (2,607 ± 1,084 vs. 1,839 ± 813; $P = 0.06$) were restored to control levels (Fig. 1*B*). Importantly, QQc increased the percentage of diabetic dEPC-CFUs (the EPC population that most readily forms new vessels) more than three-fold (17.8 ± 8.8 vs. 58.2 ± 12.7%; $P < 0.01$) (Fig. 1*C* and *D*).

QQc restores tubular formation of diabetic progenitor cells. Organization of endothelial cells in a three-dimensional network of tubes is the final step of angiogenesis. Because QQc increased the rate of diabetic KSL proliferation as well as differentially increased the proportion of diabetic dCFUs, we tested the effects of QQc on diabetic KSL tubule formation in vitro. Before QQc, on matrigel, diabetic KSL cells had significantly fewer tubules per HPF than controls (17.55 ± 7.4 vs. 28.53 ± 15.4; $P < 0.01$) (Fig. 2). Moreover, the tube formation with diabetic KSL cells demonstrated significantly less tubules per HPF compared with human umbilical vein endothelial cells with no cell group, suggesting that diabetic KSL may have a negative effect on augmenting angiogenesis (21.5 ± 6.5 vs. 17.55 ± 7.4; $P < 0.05$). Although the number of tubules per HPF with DM_{QQc} KSL cells was still significantly lower (33.3 ± 8. vs. 47.1 ± 15.3; $P < 0.05$) than C_{QQc} KSL cells tubules per HPF, diabetic KSL tube formation significantly increased (17.55 ± 7.4 vs. 33.3 ± 8.0; $P < 0.01$) after QQc, and it significantly increased compared with pre-QQc control KSL cells (33.3 ± 8.0 vs. 28.53 ± 15.4; $P < 0.05$)

QQc enhances expression of vasculogenic and wound healing factors. Because QQc increased the rate of diabetic KSL proliferation, differentially increased the proportion of diabetic dEPC-CFUs, and increased the tubule-forming potential of diabetic KSL cells, we tested the effects of

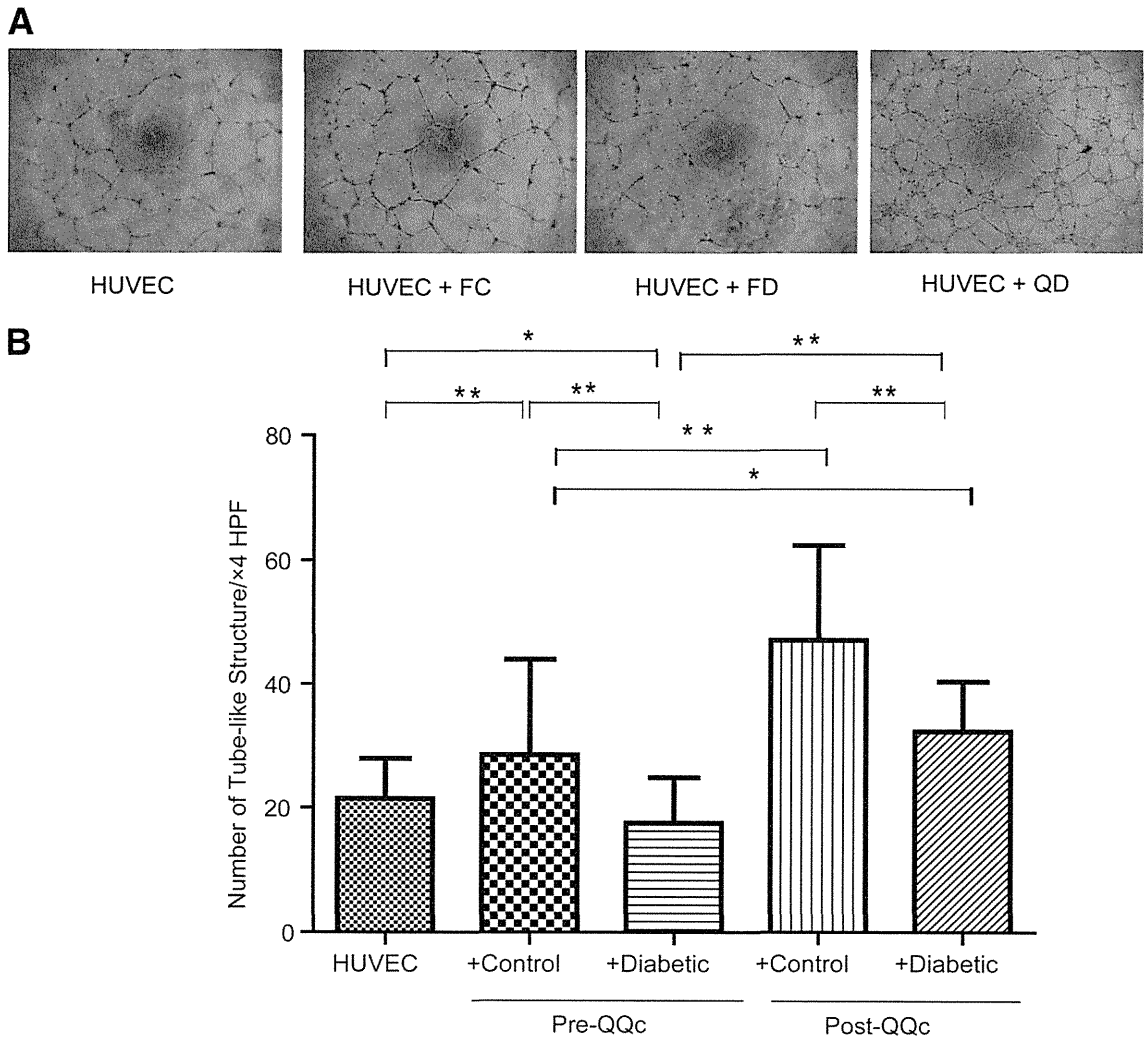

FIG. 2. QQc restores tubular formation of diabetic progenitor cells. *A*: Representative features of tube formation assay of human umbilical vein endothelial cells (HUVECs) by coculturing with presence or absence of pre-QQc and post-QQc control and diabetic cells (4× magnification). The ratio of HUVEC:KSL cells is 1×10^4:3×10^3 (10:3). *B*: Graph of the numbers of tubules formed in each group. $n = 10$ wells/group. *$P < 0.05$; **$P < 0.01$. FC, freshly isolated control cells; FD, freshly isolated diabetic cells.

QQc on diabetic KSL gene expression. After QQc, diabetic KSL cells increased their expression of wound healing–related growth factor genes endothelial growth factor, fibroblast growth factor-2, and fibroblast growth factor-7 and vasculogenesis-related genes vWF, CD29, and Flk-1 (Fig. 3). Although all key wound healing–related factors increased after QQc, endothelial growth factor production increased 3.5-fold in control KSL cells and 8.3-fold in diabetic KSL. Among the vasculogenesis-related genes, the expression of vWF increased by 8.3-fold and 6.7-fold in control and diabetic KSL, respectively, post-QQc. The expression of Flk-1 in C_{QQc} KSL remarkably increased (32.7-fold), and in DM_{QQc} KSL cells were increased 2.5-fold.

In addition to the upregulation of key wound healing and vasculogenic genes, KSLs also increase their expression of CD29/integrin β-1, an integrin unit associated with the angioblastic growth cone during vasculogenesis. After QQc, *CD29* expression in both C_{QQc} and DM_{QQc} KSL cells increased significantly (2.3-fold for control and 1.9-fold for diabetic; $P < 0.05$). Moreover, the expression of *CD29* in DM_{QQc} KSL cells was not significantly different from *CD29* expression in C_{QQc} KSL cells.

Post-QQc diabetic progenitor cell therapy accelerates wound closure. To reduce the number of confounding variables that might affect EPC function during wound closure, we tested pre-QQc and post-QQc diabetic and control KSL-adoptive cellular therapy in wounded euglycemic mice. Adoptive cellular therapy with pre-QQc diabetic KSL cells had little impact on wound healing compared with PBS treatment on day 7 (26.1 ± 3.0 vs. 30.7 ± 1.9%; $P < 0.05$), day 14 (61.5 ± 5.6 vs. 70.1 ± 3.5%; $P = 0.50$), day 18 (70.0 ± 13.6 vs. 87.4 ± 11.1%; $P = 0.6$), or day 21 (83.5 ± 5.0 vs. 89.7 ± 5.5%; $P = 0.05$) (Fig. 4*A* and *B*). In marked contrast, adoptive transfer of DM_{QQc} KSL cells accelerated the percent wound closure compared with pre-QQc diabetic treatment on day 14 (81.3 ± 8.7 vs. 61.5 ± 20.3%; $P < 0.05$), day 18 (70.0 ± 13.6 vs. 97.7 ± 4.0%; $P < 0.01$), or day 21 (83.5 ± 5.0 vs. 89.7 ± 5.5%; $P < 0.05$) (Fig. 4*A* and *B*). Moreover, the percent wound closure achieved with adoptive transfer of DM_{QQc} KSL cells was not significantly different than the percent wound closure achieved with adoptive transfer of C_{QQc} KSL on day 14 (81.3 ± 7.2 vs. 89.98 ± 7.7%; $P < 0.05$), but it was not significantly different on day 18 (97.7 ± 4.0 vs. 99.1 ± 1.5%; $P = 0.9$) or day 21 (94.4 ± 1.6 vs. 100 ± 0%; $P = 0.3$) (Fig. 4*A* and *B*).

Post-QQc adoptive diabetic progenitor therapy enhances wound vascularization and collagen maturation. To understand how QQc improved diabetic KSL-mediated wound closure, we measured wound vascularization and collagen maturation. Interestingly, wounds injected with QD KSL cells showed significantly higher CD31 counts compared with the freshly isolated diabetic KSL treatment group and PBS (13.8 ± 1.8 vs. 8.6 ± 0.9 vs. 7.2 ± 0.8; $P < 0.01$) starting at day 7. On day 21, the vascularity in the post-QQc diabetic KSL treatment groups significantly increased compared with freshly isolated control and diabetic KSL treatment groups, as well as compared with the PBS control group (25.5 ± 1.7 vs. 15.0 ± 1.8 vs. 18.0 ± 1.2 vs. 11.5 ± 1.0; $P < 0.05$). Interestingly, post-QQc KSL treatment groups showed a rapid increase in vascularity after injection, as compared with the relatively delayed response in the freshly isolated KSL treatment group (Fig. 5*A* and *B*).

On day 21, the percentage of mature collagen as assessed by Van Gieson staining in the wounds treated with post-QQc diabetic KSL cells (58 ± 11%) was greater compared with wounds treated with freshly isolated control (43 ± 14%) and diabetic KSL cells (38 ± 3%) and PBS (33 ± 7%; $P < 0.01$ and $P < 0.01$, respectively) (Fig. 6*A* and *B*).

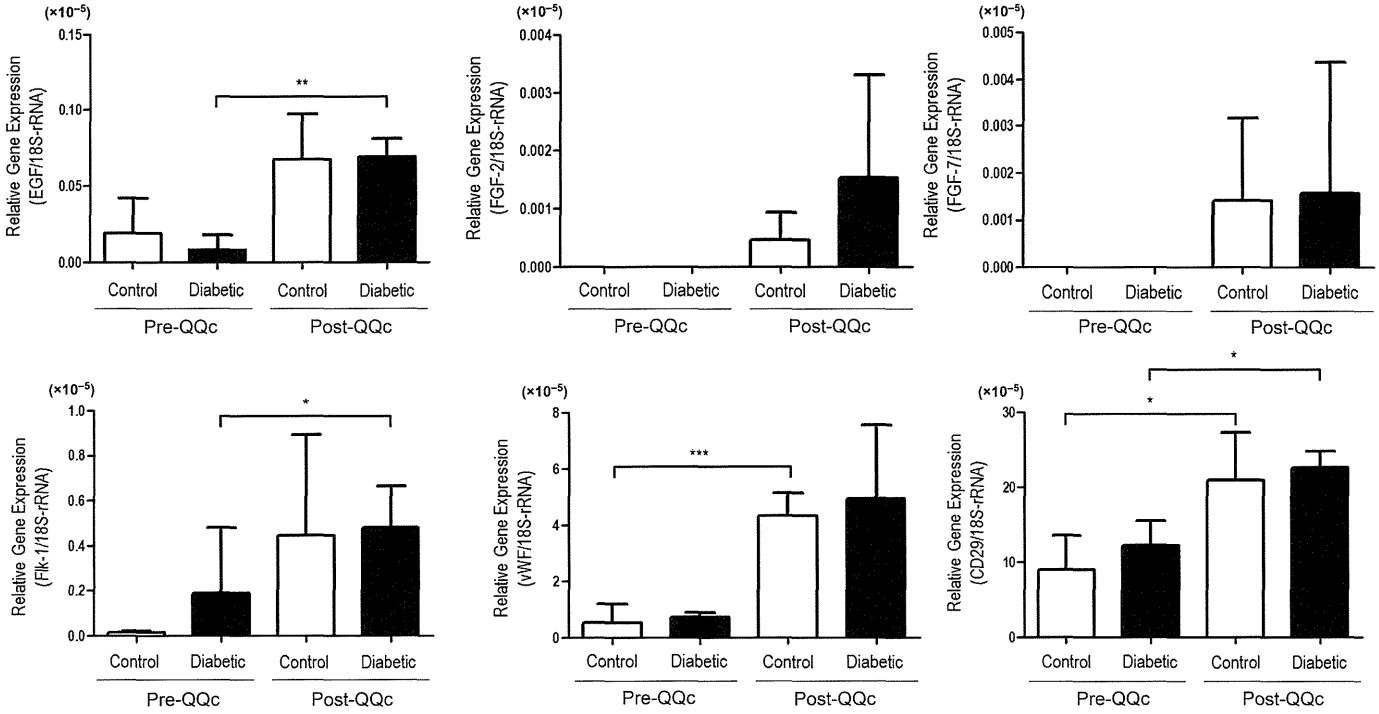

FIG. 3. QQc enhances expansion of vasculogenic and wound healing factors. The total RNA were prepared from pre-QQc and post-QQc cells from control and diabetic mice KSL cells. The gene expression levels of proangiogenic growth factors were estimated by real-time PCR, and the data were shown as the relative gene expression of the target genes vs. 18S rRNA. The target genes of quantitative PCR were EGF, FGF-2, FGF-7, vWF, CD29, and Flk-1. The data are shown as means ± SD. $n = 4$. *$P < 0.05$; **$P < 0.01$; ***$P < 0.001$. Flk-1, VEGFR-2 (KDR/Flk-1).

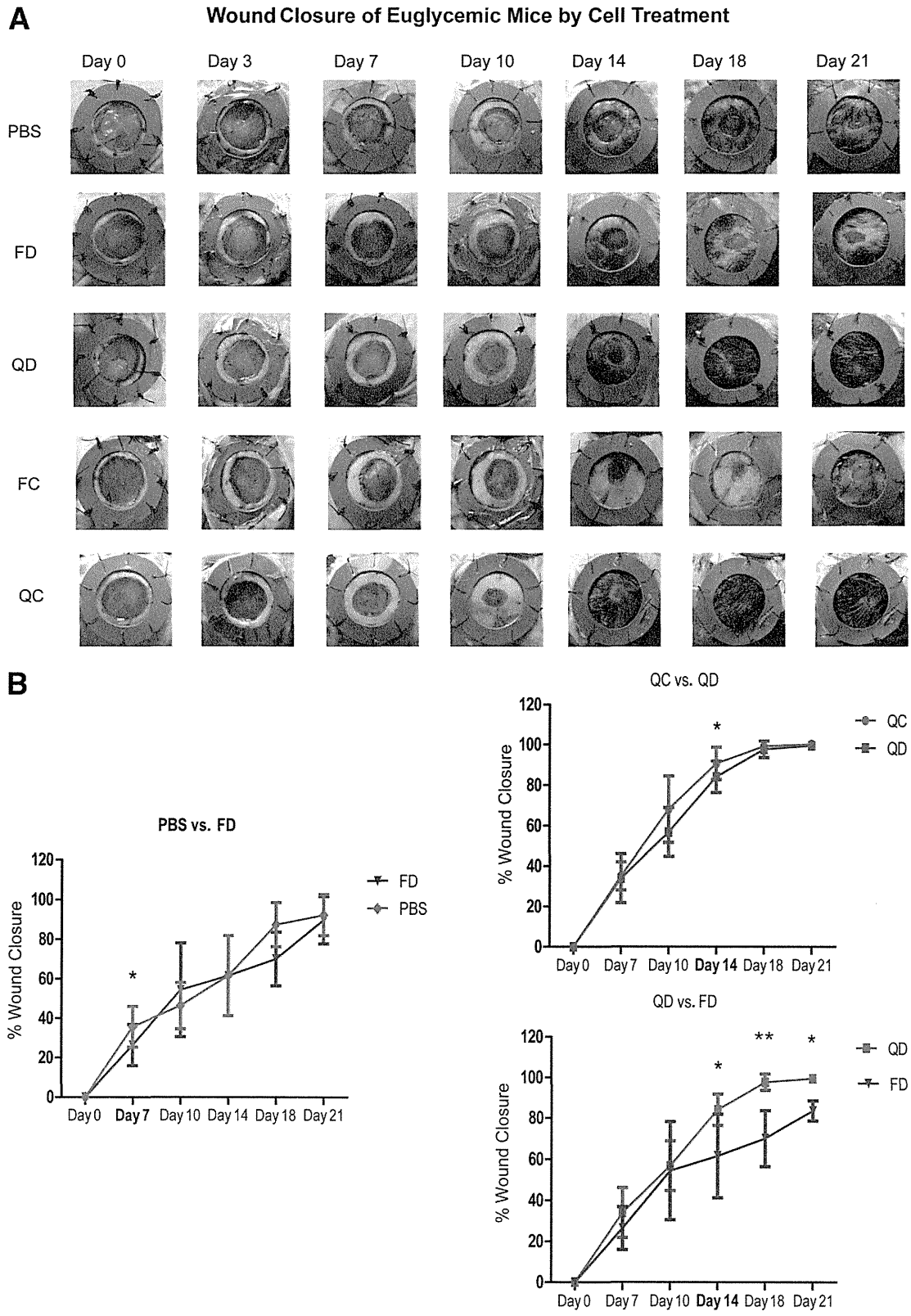

FIG. 4. Post-QQc adoptive diabetic progenitor cell therapy accelerates wound healing. *A*: Representative images show wound healing in euglycemic mice treated with PBS, pre-QQc, and post-QQc control and diabetic cells. Wounds were photographed at the times indicated from day 0 to day 21. *B*: The graphs show the comparison of percent wound closure between PBS and freshly isolated diabetic cell (FD)-treated group (*left*), post-QQc control cell (QC)-treated group, QD-treated group (*top right*), and QD-treated and FD-treated group (*bottom right*). *$P < 0.05$; **$P < 0.01$. FC, freshly isolated control cell.

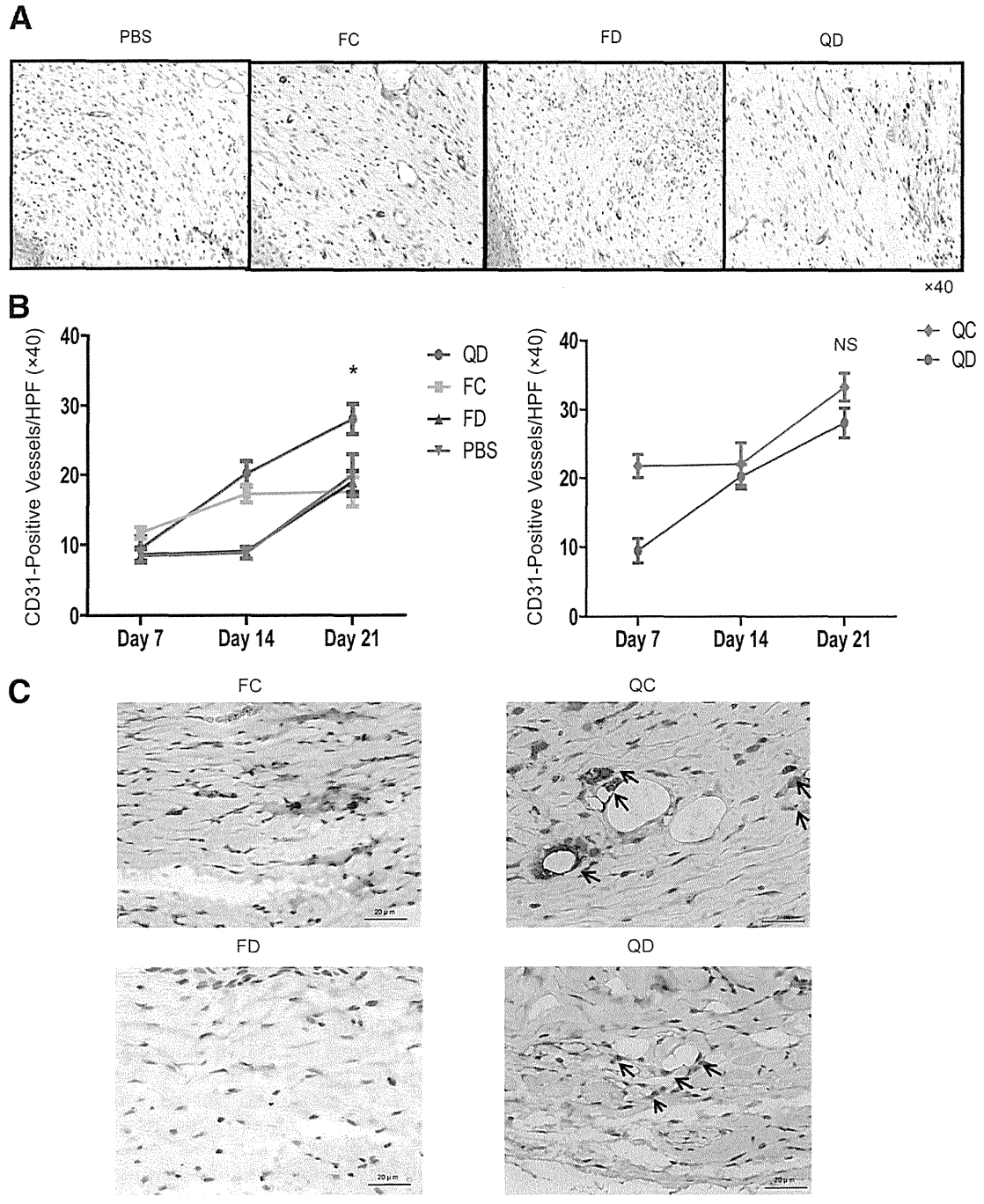

FIG. 5. Post-QQc diabetic progenitor cell therapy enhances wound vascularization. *A*: Representative immunohistochemistry staining of CD31 to evaluate vascular density in the wounds of PBS-treated, freshly isolated control cell (FC)-treated, freshly isolated diabetic cell (FD)-treated, and QD-treated groups at day 21 (×40). *B*: The graphs show the CD31-positive vessels per HPF at days 7, 14, and 21. *Left graph* shows the comparison between QD-treated and FC-treated, FD-treated, and PBS-treated groups. *Right graph* shows the comparison between post-QQc control cell (QC)-treated and QD-treated groups. $^*P < 0.05$. *C*: Representative immunohistochemistry double staining of GFP (brown) and vWF (red). The arrows point to the vessels with positive double staining. ×60 scale bar = 20 μm. The staining demonstrates that GFP/vWF double-stained vessels are only observed in the post-QQc control- and diabetic cell-treated wounds. GFP-positive cells observed more in the QC treated group. NS, not significant.

Post-QQc diabetic progenitor cells have high potential for direct vasculogenesis. To identify whether the increased vascularity is attributable to differentiation of injected post-QQc KSL cells or is attributable to increased numbers of resident endothelial cells, we injected pre-QQc and post-QQc GFP control and diabetic KSL cells in the wound and identified the GFP and vWF costaining cells. As a result, GFP-positive cells costained with vWF were only identified in the post-QQc control and the diabetic cell-treated groups at day 21. Comparing post-QQc control and diabetic cell-treated groups, the post-QQc control cell-treated group showed higher numbers of GFP cells incorporated into the vasculature, suggesting higher vasculogenesis of post-QQc control KSL cells (Fig. 5C).

Post-QQc diabetic progenitor cell therapy increases cellular proliferation in the wound. To study the effects

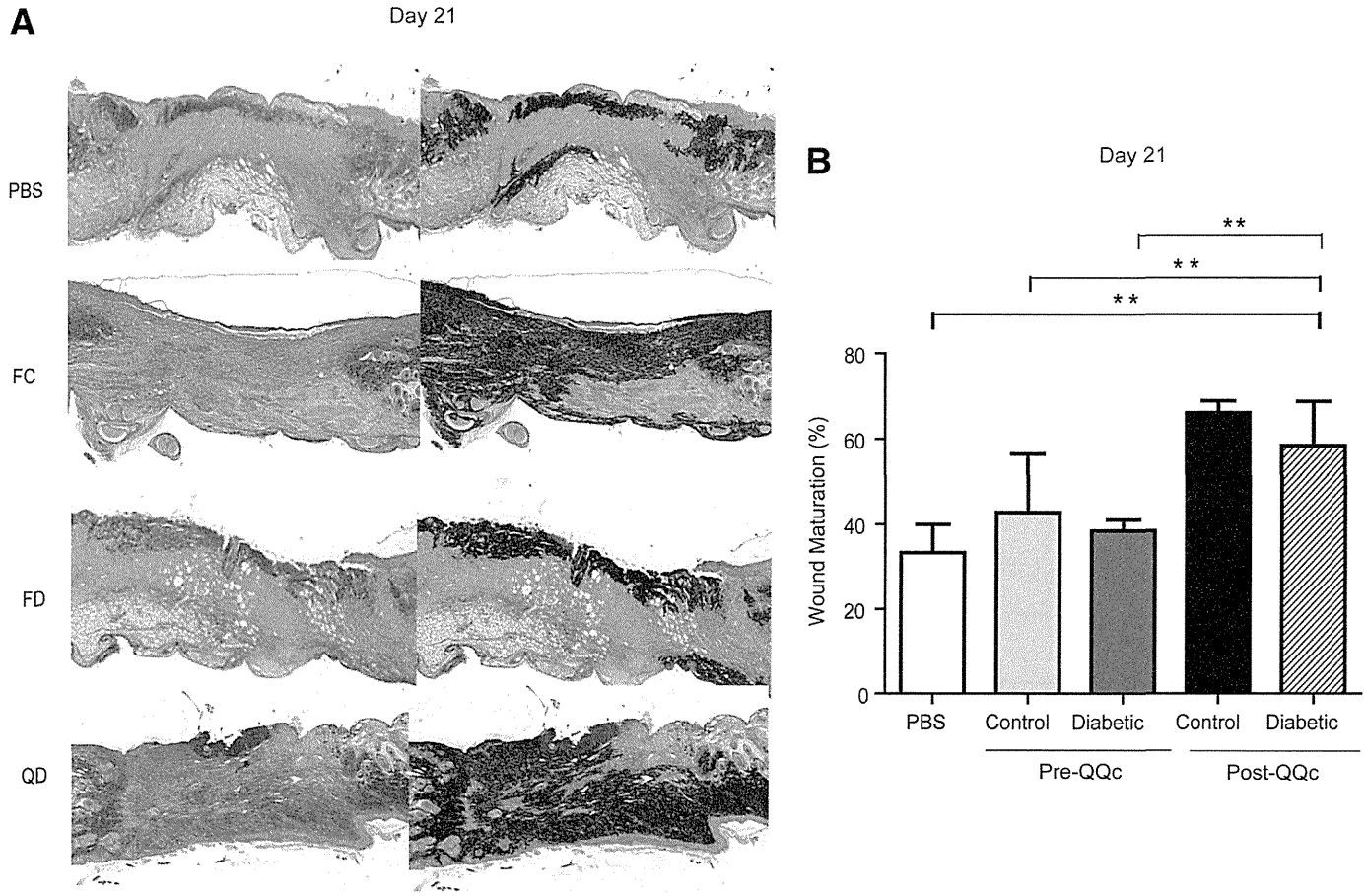

FIG. 6. Post-QQc diabetic progenitor cell therapy enhances the percentage of mature collagen in the wound. *A*: Representative Van Gieson staining demonstrating mature collagen staining in PBS-treated, freshly isolated control cell (FC)-treated, freshly isolated diabetic cell (FD)-treated, and QD-treated groups on day 21 (×10). *B*: The graph shows the percentage of mature collagen in wounds treated with PBS, FC, FD, and QD cells on day 21. **$P < 0.01$.

of QQc-expanded diabetic KSL cells on native cells in the wound, we measure fibroblastic proliferation in situ. After adoptive QD KSL treatment, wound fibroblastic proliferation peaked early and declined significantly from day 7 to day 21 in the groups treated with freshly isolated control KSL cells (795 ± 221 vs. 247 ± 86 cells/field; $P = 0.044$) and post-QD KSL cells (761 ± 171 vs. 238 ± 141 cells/field; $P = 0.011$). Contrarily, there was no increase in cellular proliferation in wounds treated with freshly isolated diabetic KSL cells (664 ± 321 vs. 534 ± 116 cells/field; $P = 0.41$) or PBS (621 ± 122 vs. 672 ± 278 cells/field; $P = 0.31$) (Fig. 7).

Function of post-QQc diabetic progenitor cells is deteriorated in glycemic diabetic wounds. The in vivo efficacy of post-QQc diabetic KSL cells also was tested in STZ-induced glycemic murine diabetic wounds. As a result, post-QQc KSL cells indicated significant percent wound closure compared with pre-QQc KSL cells and PBS on day 14 (73.60 ± 3.69 vs. 55.02 ± 3.61 vs. 58.98 ± 5.86%; $P < 0.05$) and day 21 (96.34 ± 1.52 vs. 82.29 ± 4.72 vs. 84.01 ±2.28%; $P < 0.05$) (Fig. 8). However, there was no significant difference between the wound closures between pre-C_{QQc} KSL, pre-DM_{QQc} and post-DM_{QQc} KSL, and PBS at all times. Although post-DM_{QQc} KSL can accelerate wound healing and possess the restored vasculogenic potential in euglycemic in vivo conditions, these data suggest functional limitation of post-DM_{QQc} KSL function in glycemic diabetic condition.

DISCUSSION

Current diabetic wound treatment hinges on patient education, prevention, and early diagnosis. Once a wound has developed, however, invasive therapies are costly and noninvasive therapies are less effective. Ultimately, because current treatments do not correct the underlying pathophysiology, many patients experience untoward complications and require amputations. Although investigators have long focused on the detrimental effects of elevated blood glucose on diabetic wound healing, recent data suggest that diabetic impairment of EPC function has a secondary effect on diabetic wound healing (5,34). This latter point is highlighted in the results of our recent clinical trial (24). By injecting autologous granulocyte colony-stimulating factor–mobilized peripheral blood EPCs into the nonhealing wounds of diabetic patients, we found that successful wound healing correlated with the vasculogenic function of transplanted EPCs. Moreover, we discovered that autologous EPC therapy has two inherent limitations: low EPC cell number and low vasculogenic function.

In an effort to overcome the limitations of autologous EPC therapy in diabetic patients, we studied the effect of QQc diabetic EPC ex vivo expansion on wound healing. In our study, mouse BM KSL cells were used as an EPC-enriched population based on a recent study reported by